International Conference On Emerging Trends in Engineering and Management Research
NGSPM's Brahma Valley College of Engineering & Research Institute, Anjaneri, Nashik(MS) (ICETEMR-16)
23rd March 2016, www.conferenceworld.in ISBN: 978-81-932074-7-5

FAULT TOLERANT HEV POWER TRAIN

Priyanka Sonawane[1], Sarita Jadhav[2], Prof. Sayali Patil[3]

T.E.Electrical[1,2] Scholar, B.V.C.O.&R.I., NASHIK,(India)

Professor of Electrical Dept.[3], B.V.C.O.E.&R.I., NASHIK, (India)

ABSTRACT

This paper presents a fault-tolerant design of powertrain series hybrid electric vehicle (SHEVs).Through introduction of a common redundant phase leg for the rectifier, the inverter and the buck/boost converter of the standard drive system, a design with minimal cost increase has been realized. The new topology features superior fault-handling capability, post-fault operation at rated power throughput, and improved reliability. The operating principle and control strategy of the fault-tolerance are presented. A Markov reliability model is constructed to quantitatively assess the reliability of the proposed powertrain. Numerical simulation based on a Saber model has been conducted and the results have verified the feasibility and performance of the proposed SHEV drive system with fault-tolerant capability.

Keywords: Hybrid Electric Vehicle (HEV), Series (HEV) powertrain, Fault tolerant, Markov model, Saber model,Reliability.

I.INTRODUCTION

Hybrid electric vehicles (HEVs), with their excellent mile-per-gallon performance, have been considered as a pivotal technology to mitigate concerns over the rapid rising of petroleum cost, increasingly worsening air pollution and global warming associated with greenhouse gas emission [1]. A literature survey suggests that the major research effort has been focused on power electronic converter topologies and motor control systems related to HEVs while significantly less attention has been devoted to the reliability and fault mitigation of HEVs' powertrains. In fact, aggregation of many power electronic devices into drive systems of vehicles adversely affects reliability of the overall system [2]. The reduced reliability of HEVs not only discounts fuel-saving premium, but also increases repair time and repair cost. In light of safety concerns, faults that occur in electric drives for propulsion systems of HEVs can be critical since an uncontrolled output torque exerts adverse impact on the vehicle stability, which can ultimately risk the passenger's safety. Therefore, a fault tolerant operation even with partial functionality (commonly known as *limping-home function*) is desirable [3]. This paper compares and contrasts several competitive candidates for fault-tolerant designs employed in HEVs electrical machine driving systems in terms of performance and cost. However the dc-link capacitors have to be oversized to absorb fundamental load currents under faulted conditions. A fault-tolerant electric drive system for series hybrid electric vehicles (SHEVs) is proposed to overcome the limitations that are associated with the existing topologies. The operating principle of the proposed topology is explained in Section II. The salient reliability metrics of the existing and proposed SHEV powertrain are assessed and compared in Section III. Section IV presents the time-domain simulation results that verify the control of the proposed topology. Finally summary and brief discussions conclude this paper.

II. PROPOSED SHEV POWERTRAIN WITH FAULT-TOLERANT

The standard SHEV drive system consists of a three-phase rectifier, a three-phase inverter and a bidirectional buck/boost dc/dc converter. Faults on any power device can cause the system to shut down. A fault-tolerant drive system for SHEV is proposed to reduce unexpected stoppages caused by faults of semiconductor devices. As shown in Fig. 1,the newly proposed system is composed of a standard SHEV powertrain, are Dunant phase leg, connecting devices and fault-isolating components. The system provides a redundancy not only to the motor-drive inverter, but also to the rectifier and the buck/boost converter. Under the conditions of open-switch or short-switch failure of any switch in these three converters, the system can maintain an uninterruptible and long-term post-fault operation without compromising the power throughput. Since three converters share one redundant leg, the relative cost of the system is lower than other four-leg fault-tolerant inverters that have been reported in literature for motor drives.

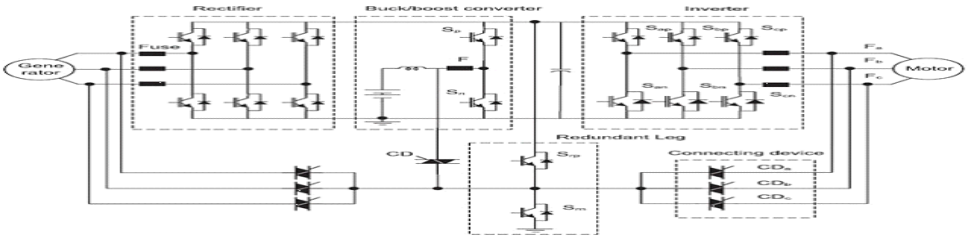

Fig.1 Series HEV Powertrain with Integrated system[3]

A. Isolating and Connecting Devices

The short-switch fault is one of the most common types of motor driving inverter faults. In case of a short-circuit failure on any switch, one phase of the motor will be connected permanently to the positive or negative rail of the dc bus, which results in the pulsating electromagnetic torque. A device is needed to isolate the faulted switch from the overall system. Herein, a fast-acting fuse is utilized to fulfill this function. For instance, in the case that a short-circuit failure occurs on the upper switch *S*ap of the *a*-phase leg of the inverter, the *a*-phase of the motor will be directly linked to the positive rail of the dc bus, as shown in Fig. 1. The resultant *a*-phase current becomes uncontrolled. After this fault is successfully isolated through clearing the fuse *F*a, further remedial measures can be employed to restore the normal operation of the system. Since the inverter, the rectifier and the buck/boost converter share the same backup leg, a connecting device is necessary to connect the standard phase legs to the redundant one. These devices shall be able to block bidirectional voltage and conduct alternate current. The connecting devices for the inverter and the rectifier commutate once every fundamental cycle, so a low-speed low-cost ac switch suffices to handle this task. Although the buck/boost converter may operate in the discontinuous mode and consequently the connecting device has to commutate at the switching frequency, the same low-speed ac switch can still be applied to this converter as the connecting device, due to the inherent zero-current turning-off characteristic of the discontinuous-mode buck/boost converter.

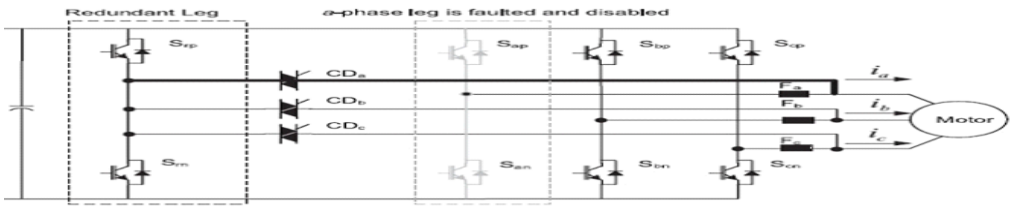

Fig. 2. Power circuit of the dc/ac part after its *a*-phase leg is faulted[3]

B. Open-Switch Fault and Control Strategy

The new SHEV drive system can squarely handle open-circuit or misfiring faults in one or two IGBTs in the same leg of the three converters. When only one power device fails, the key to achieve the fault-tolerant operation is to isolate the faulted component and then reconfigure the structure and control strategy of the drive system. The specific control scheme is elaborated as the following for the instance of the failure in switch *S*ap of the inverter. Fault isolation is implemented by permanently disabling the gating signals to both the faulted and the non-faulted switches *S*ap and *S*an in the *a*-phase leg with reference to Fig. 1. Then the connecting ac switch *CD*a is activated, and the control signals of the faulted leg are subsequently routed to the two result, the load current *i*a that originally flowed through the faulty leg is diverted to the corresponding switches *S*rp and *S*rn in the redundant leg. As a redundant one. Since this actuation does not fundamentally change the topology of the converters (rectifier, inverter or buck/boost converter), pulse width modulation (PWM) techniques and control algorithms can remain unchanged, which results in the post-fault operation of the system rather similar to its normal state. The only operational alternation amounts to the additional conduction loss of an ac switch. Fig. 2 shows the reconfigured power circuit of the dc/ac inverter after one switch of its *a*-phase leg fails with open circuit. After the redundant leg replaces the faulty *a*-phase leg, the post-fault topology is identical to the standard three-phase inverter bridge except for the addition of the connecting device. The nearly same control strategy can be applied to failure scenarios associated with other switches.

C. Short-Switch Fault and Control Strategy

It is relatively more involved to handle short-circuit faults in general due to the need of fault isolation. Different schemes are employed to isolate short-circuit faults in switches of the dc/ac inverter and the ac/dc rectifier, and the dc/dc converter. Upon detection of a short-circuit fault in an upper or lower switch of the inverter or the rectifier, the complementary switch in the same leg is blocked immediately. Then the corresponding connecting device TRIAC and the upper or lower switch in the backup leg are activated, and thus consist of a shoot-through loop with the dc-link capacitors. Fig. 3 illustrates the short-circuit path marked by the red bold line in the case of a short-switch faults in a-phase upper switch Sap of the inverter.

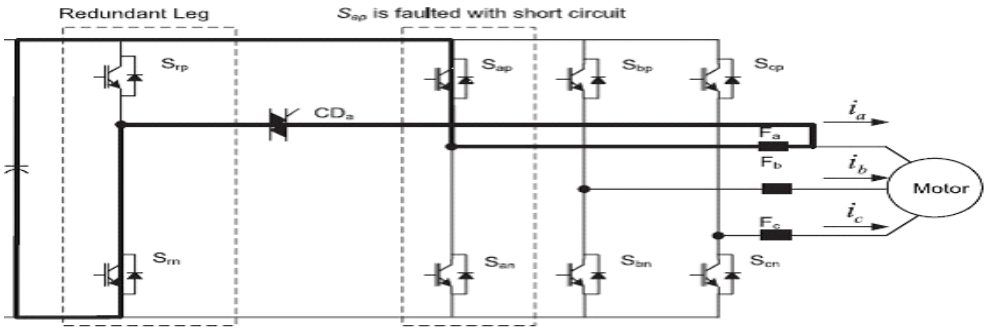

Fig. 3. The shoot-through path to blow out the fuse after the *a*-phase top switch of the inverter fails with short circuit.

The resultant large inrush current in the shoot-through loop will clear the fuse *F*a of the faulted phase. After the fuse successfully isolates the faulted phase leg from the system, the original gating signals for *S*ap and *S*an are applied to the two corresponding switches *S*rp and *S*rn in the backup leg. The control strategy for the post-fault operation is the same as the cases of the open-switch faults. When the upper switch of the buck/boost converter fails to open during buck-mode operation, the battery pack is connected to the positive rail of the dc bus through the inductor. As a result, the large battery charging current will clear the fuse. In the case of a short-circuit fault in the lower switch during boost-mode operation, the battery is shorted to the negative rail of the dc bus through the inductor. The resultant larger battery discharge current than the normal value clears the fuse. Once the faulted switch is isolated by the blown fuse, the connecting device TRIAC is activated, and the control signals are applied to the backup one. No further change is needed.

D. Fault Diagnosis

Fault detection and identification are two important steps to prevent fault propagation and to maintain proper post-fault operation of the system. Various solutions to fault diagnosis of inverters for motor drives have been proposed [10-12]. These methods can be classified into two categories. The first category is mainly based on the analysis of the inverter output currents, which features the low cost and low speed. Another category of solutions involves gate drive signals, voltage and current across/through the switches for fault diagnosis. The latter can accomplish fault detection in one to several switching cycles. The former ac-based methods of fault detection cannot be applied to the buck/boost converter. Nowadays, the smart drivers of IGBTs often have embedded voltage-sensing and current-sensing circuits. These integrated capabilities reduce complexity and cost of the fault diagnosis. Herein the second solution is adopted to identify the faulted devices. Table I shows the logic of fault diagnosis for the upper switch in the *b*-phase leg of the inverter. For instance, when the gating signal is disabled, but the sensed voltage across the device is low and the current flowing through the switch is high, a short-circuit failure of the device is thus detected. Since the switches are identical, the scheme of fault diagnosis can be applied to other switches as well.

III. RELIABILITY ANALYSIS OF THE FAULT-TOLERANT SHEV POWER TRAIN

The reliability of the system is closely related to the repair cost and repair time. This section quantitatively assesses the reliability of the proposed and the standard SHEV drive

 ISBN: 978-81-932074-7-5

Table I Fault Detection Logic Of Sap

Driving signal of Sbp	Driving signal of Sbn	Voltage across Sbp	Current through Sbp	Fault detection
on	off	*H*	*L*	Sbp OC fault
on	off	*L*	/	Normal
off	/	*L*	*H*	Sbp SC fault
off	off	*L*	*H*	Normal

systems. In the assessment of the new drive system's reliability improvement, only semiconductor devices IGBTs and TRIACs are considered to demonstrate the methodology although inclusion of other passive components is rather straightforward.

A. Components Failure Rates

The reliability handbook MIL-217F provides an extensive database of various types of parts. Therefore, it is widely accepted and frequently utilized to determine reliability of various electronic equipment. In order to make use of the failure rate models of components from the handbook, the following operating conditions have been assumed:

1) The power ratings are 100 kW for the inverter, 70 kW for the rectifier, and 30 kW for the buck/boost converter;

2) The dc-link voltage is 250–600 V, and, therefore, devices with the rating of 1200 V/600 A are selected;

3) The junction temperature of devices is 150 ◦C;

4) Reliability of IGBTs and TRIACs are considered;

5) Failure rates of components in inactive mode equal zero. The reliability model of TRIAC is determined by;

$$\lambda\text{SCR} = \lambda b \pi T\, \pi R \pi S\, \pi Q \pi E$$

where,

λb: base failure rate;

πT: temperature factor;

πR: current rating factor;

πS : voltage stress factor;

πQ: quality factor;

πE: environmental factor.

The MIL-HDBK-217F contains no reliability data about IGBTs. In consideration of the similarity between the internal structures of IGBTs and MOSFETs, the failure rate model of MOSFTs is chosen to estimate failure rates of IGBTs. Hence, the failure rate of IGBTs can be expressed as

$$\lambda\text{IGBT} = \lambda b \pi T\, \pi A \pi E\, \Pi q$$

where πA is application factor while the other parameters have been explained in.

B. Fundamentals of Markov Reliability Model

At the system level, Markov chain is an effective approach to evaluating the reliability of fault- tolerant systems. This approach can cover many features of redundant systems such as sequence of failures, failure coverage, and state-dependent failure rates.Markov model can be utilized to estimate various reliability metrics such as failure rate, mean time to failure (MTTF), reliability, and availability among others. Firstly a stochastic state variable $X(t)$, $t > 0$ is defined, which represents states of the system. At time instant t, the probability $Pi(t)$ for the system to be in the *ith* state is expressed as

$$Pi(t) = P\{X(t) = i\}.$$

If the system is in the *ith* state at time t, the probability $Pij\ (t)$ that the system transitions to the *jth* tate after a time interval

Δt is,

$$Pij\ (t) = P\{X(t+\Delta t) = j | X(t) = i\}.$$

The transition rate αij that denotes the probability of system transitioning from state i to state j during the time unit is determined by,

$$\alpha_{ij} = \lim_{\Delta t \to 0} \frac{P_{ij}(t)}{\Delta t}.$$

.

Transition rates of the fault-tolerant system are analogous to the failure rates and repair rates of non-redundant systems. The transition amongst different states of a system is caused by failure and repair events of components. Fig. 5 illustrates the state transition diagram for the simple case of two states. If a system has k states, then the state equation is expressed as [41].

$$\frac{d}{dt}\begin{bmatrix} P_0(t) \\ P_1(t) \\ \vdots \\ P_k(t) \end{bmatrix} = \begin{bmatrix} -\alpha_{00} & \alpha_{01} & \cdots & \alpha_{0k} \\ \alpha_{10} & -\alpha_{11} & \cdots & \alpha_{1k} \\ \vdots & \vdots & \cdots & \vdots \\ \alpha_{k0} & \alpha_{k1} & \cdots & -\alpha_{kk} \end{bmatrix} \begin{bmatrix} P_0(t) \\ P_1(t) \\ \vdots \\ P_k(t) \end{bmatrix}$$

The probabilities that the system is in each state at time t can be obtained by solving the state equation. Probabilities $P0\ (t)$, $P1\ (t)$, . . . , $Pm(t)$, correspond to normal or degraded states 0, 1, . . .,m, while probabilities $Pm+1(t)$, $Pm+2(t)$, . . . , $Pk\ (t)$ correspond to failed states m +1, m + 2, . . . , k. The reliability function of the system is the sum of probabilities functions of all functional (non-failed) states, which is mathematically expressed as,

$$R(t) = \sum_{i=0}^{m} P_i(t).$$

C. Reliability Evaluation of the SHEV Driving System

Markov reliability model is adopted to assess the reliability of the fault-tolerant SHEV drive system. In order to reduce the order of the state equation, all devices with the same operating states and transition processes are treated as one subsystem. The system can be divided into two subsystems: one including all IGBTs and the other including all TRIACs. Repair processes have not been considered in this study. The system has three states:

State 0: All devices in the three converters of the standard drive work normally, and the redundant and connecting devices are in inactive mode;

State 1: One IGBT fails, and the redundant leg and correspondent connecting device TRIAC are activated; and

State 2: Two components (IGBTs or the combination of a TRIAC and an IGBT) fail, and the system shuts down.

A short-switch or open-switch failure of any one of the IGBTs in the rectifier, the inverter or the buck/boost leads to transition of the system to State 1 from State 0. Since all IGBTs are assumed to have the same junction temperature, the transition rate $\alpha 01$ is the sum of failure rates of all operating IGBTs. Transition between State 1 and State 2 are triggered by a failure of one IGBT in remaining healthy and the redundant legs or the TRIAC that is in active mode. The transition rate $\alpha 12$ comprises the failure rates of operating IGBTs and TRIAC. It is worth noting that only one TRIAC operates in State 1. From, the state equation of the SHEV system can be obtained as

$$\frac{d}{dt}\begin{bmatrix} P_0(t) \\ P_1(t) \\ P_2(t) \end{bmatrix} = \begin{bmatrix} -\alpha_{01} & 0 & 0 \\ \alpha_{01} & -\alpha_{12} & 0 \\ 0 & \alpha_{12} & 0 \end{bmatrix} \begin{bmatrix} P_0(t) \\ P_1(t) \\ P_2(t) \end{bmatrix}.$$

With the assumption that the probabilities that the system is in the functional states at time *t*, the reliability of the system can be obtained as

$$R(t) = P0\ (t) + P1\ (t)$$

Fig. 4 illustrates the reliability functions of the proposed fault tolerant powertrain and the standard SHEV powertrain. It is evident that the reliability of the proposed drive system is substantially higher than that of the standard one due to the presence of the redundant phase leg. The MTTF is another important index indicating the reliability of a system, which is related to the reliability function by the following:

$$\text{MTTF} = \int_0^{+\infty} R(t)dt.$$

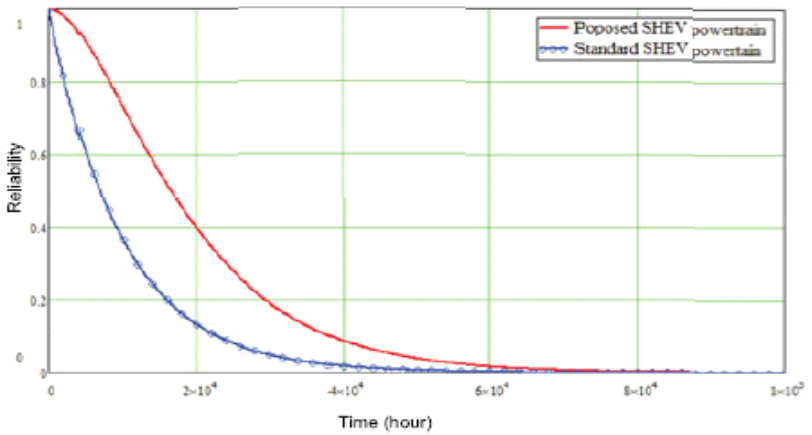

Fig. 4. Reliability functions of the proposed and standard SHEV powertrains.

Table II MTTF of the proposed and standard SHEV powertrains

Topology	MTTF
Standard powertrain	9.871×10^3 hours
Proposed powertrain	1.966×10^4 hours

Table III Specification and parameters of simulation model

Parameter	Value
DC-link voltage	55 V
Fundamental frequency	60 Hz
Switching frequency	5 kHz
Modulation index	0.8
Load resistance	5 Ω
Load inductance	9 mH

In Table II, MTTFs of the new fault-tolerant and the standard SHEV drive trains are listed. The significantly improved MTTF demonstrates the superior reliability performance of the new topology. The operating time of the proposed fault-tolerant topology has been improved twice as much as that of the standard SHEV drives system.

IV. SIMULATION RESULTS

The post fault operating performance of the proposed SHEV driving system is verified by time-domain simulation by use of Saber. The simulation is based on the fault-tolerant design of SHEV powertrain as shown in Fig. 4. Because the fault diagnosis scheme and postfault remedial strategy are identical for the inverter, the rectifier and the buck/boost converter, only the faults on the dc/ac inverter that directly drives the motor and the corresponding postfault performance are investigated. The simulated system model consists of the proposed fault-tolerant three-phase inverter and an resistance–inductance load. The detailed specification and parameters of the system are tabulated in Table III. Fig. 5 shows the transition process of the system from the normal operating condition to short-switch fault condition of the inverter. At the instant of 0.05 s, a short-switch.

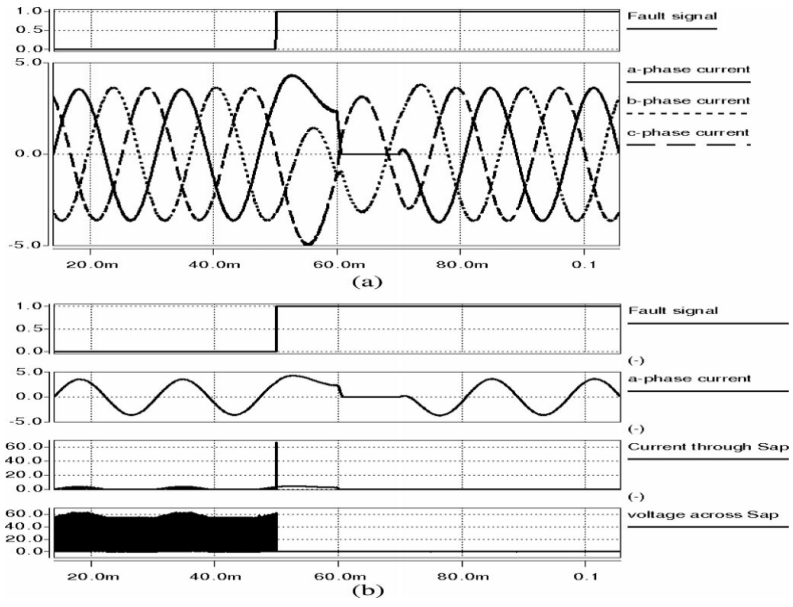

Fig. 5. Simulation results based on the second fault-tolerant topology in case of short-switch fault of *S*ap : (a) fault signal and the three-phase load currents and (b) fault signal, the load current of the faulted phase, the current through the faulted switch, and the voltage across the faulted switch.

Fault occurs to the top switch *S*ap of the *a*-phase leg. A much larger than-normal current through the faulted device substantially results. The immediate remedial action should be taken to avoid fault propagation. It further verifies that the slow-acting fault-diagnosis methods based on the output current or voltage of the inverter are not suitable for identifying short-switch fault. The fault-detection method presented in this paper features a very short delay of approximate 1 μs that is caused by the analog components and a low-pass filer in the fault-detection circuit. At time instant t = 50 ms, a short circuit occurs to *S*ap. Once the fault is detected, the gating signal of the bottom switch *S*an in the *a*-phase leg is disabled and the large current flowing through the faulted leg during the interval of fault is immediately terminated as shown in Fig. 8. Then the isolating device *Sa* is controlled to be open, and the connecting device CD*a* is triggered. At time instant t = 60 ms, the relay *Sa* is fully disconnected. And in another delay of about 10 ms, the original gating signals to both switches of the faulted leg are routed to the corresponding switches of the backup leg at t = 70 ms. Herein, the delay between time instants t = 60 and 70 ms is inserted to guarantee that the relay is fully disconnected before the redundant leg participates in operation of the system. Otherwise, the bottom switch *S*rn in the redundant leg and the faulted switch *S*ap will of open-switch fault of *S*ap :

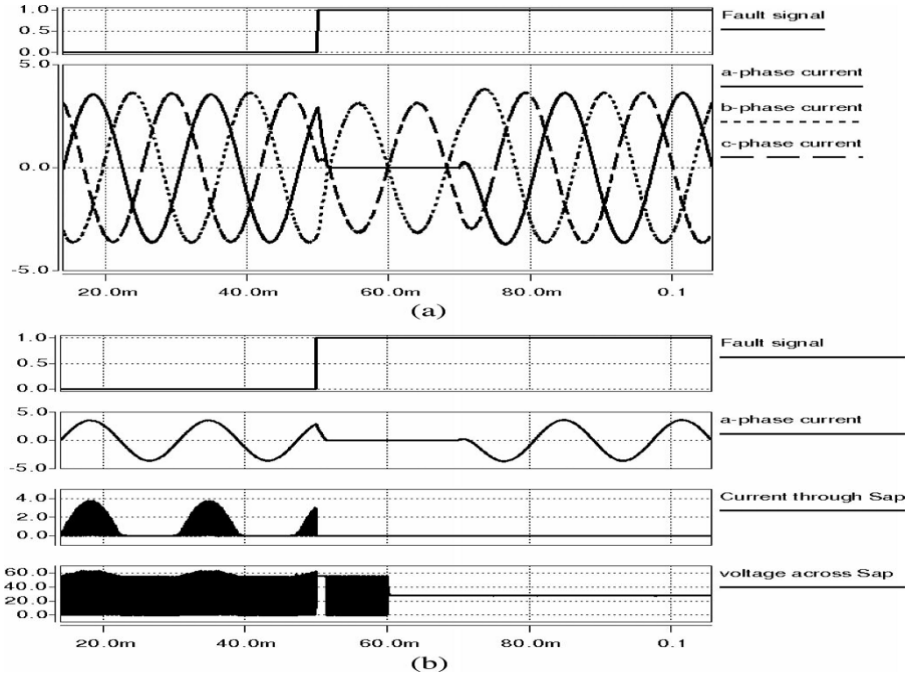

Fig. 6. Simulation results based on the second fault-tolerant topology in case:

(a) fault signal and the three-phase load currents and (b) fault signal, theload current of the faulted phase, the current through the faulted switch, and the voltage across the faulted switch.

form a shoot-through path. The postfault operation starts and normal system performance is resumed from t = 70 ms. The transition process of the open-switch fault is illustrated in Fig. 6. The fault isolation actions taken by the

controller are the same as the ones for the case of the short-switch fault except that the fault-detection logic is different, which has been explained in Section III.

V. CONCLUSION

The performance of an existing HEV was improved using the proposed HESS. Simulations of the proposed configuration and control strategy were performed in the MATLAB/Simulink simulation environment. A method for calculating the parameters of the proposed HESS was presented. The simulation results showed that with the calculated values of the parameters, the proposed HESS could satisfy the power and energy demands of DC bus with a lower capacity DC-DC converter than was required with the traditional HESS. Moreover, by different series-parallel connections in battery Hybrid and ultra-capacitor modules the efficiency and reliability of storage system can be proved.

REFERENCES

[1] M. Ehsani, Y. Gao, and A. Emadi, Modern Electric, Hybrid Electric, and Fuel Cell Vehicles: Fundamentals, Theory, and Design, (Series Power Electronics and Applications), 2nd ed. Boca Raton, FL, USA: CRC Press, 2009.

[2] O. Hegazy, J. Van Mierlo, and P. Lataire, "Analysis, modeling, and implementation of a multidevice interleaved dc/dc converter for fuel cell hybrid electric vehicles," IEEE Trans. Power Electron., vol. 27, no. 11, pp. 4445–4458, Nov. 2012.

[3] I. Aharon and A. Kuperman, "Topological overview of powertrains for battery-powered vehicles with range extenders," IEEE Trans. Power Electron.,vol. 26, no. 3, pp. 868–876, Mar. 2011.

[4] L. Ni, D. Patterson, and J. Hudgins, "High power current sensorless bidirectional 16-phase interleaved dc–dc converter for hybrid vehicle application," IEEE Trans. Power Electron., vol. 27, no. 3, pp. 1141–1151, Mar. 2012.

[5] W. Qian, H. Cha, F. Z. Peng, and L. Tolbert, "55-kw variable 3x dc– dc converter for plug-in hybrid electric vehicles," IEEE Trans. Power Electron., vol. 27, no. 4, pp. 1668–1678, Apr. 2012.

[6] M. Pahlevaninezhad, P. Das, J. Drobnik, P. Jain, and A. Bakhshai, "A ZVS interleaved boost ac/dc converter used in plug-in electric vehicles," IEEE Trans. Power Electron., vol. 27, no. 8, pp. 3513–3529, Aug. 2012.

[7] M. Pahlevaninezhad, P. Das, J. Drobnik, P. Jain, and A. Bakhshai, "A novel ZVZCS full-bridge dc/dc converter used for electric vehicles," IEEE Trans. Power Electron., vol. 27, no. 6, pp. 2752–2769, Jun. 2012.

[8] K. Chau, C. Chan, and C. Liu, "Overview of permanent-magnet brushless drives for electric and hybrid electric vehicles," IEEE Trans. Ind. Electron., vol. 55, no. 6, pp. 2246–2257, Jun. 2008.

[9] A. Tani, M. Camara, and B. Dakyo, "Energy management based on frequency approach for hybrid electric vehicle applications: Fuelcell/ lithium-battery and ultracapacitors," IEEE Trans. Veh. Technol., vol. 61, no. 8, pp. 3375–3386, Oct. 2012.

 ISBN: 978-81-932074-7-5

[10] S. Lu, K. Corzine, andM. Ferdowsi, "A new battery/ultracapacitor energy storage system design and its motor drive integration for hybrid electric vehicles," IEEE Trans. Veh. Technol., vol. 56, no. 4, pp. 1516–1523, Jul.2007.